# Identification and characterization of metal doped titania $Co^{II}$:nano-$TiO_2$ using [Co(pic)$_4$Cl$_2$]/nano-$TiO_2$

**K. Rajkumar, A. S. Ganeshraja, B. Bhavana, K. Anbalagan***

Department of Chemistry, Pondicherry University, Pondicherry 605 014, India
e-mail: kanuniv@gmail.com, Tel: +91 413 2654509

*Abstract*: - **[Co(pic)$_4$Cl$_2$] can preferably adsorb onto the surface of nanosized titania and forms an adduct, subsequently this yields surface species; TiO$_2$:Co$^{II}$. Here surface chemistry influences the implantation of the cobalt(II) ion which is due to adsorption of the complex ion on the surface of the solid. To understand the affinity of the Co(II) complex on the surface of nanocrystalline anatase, adsorption study was carried out in neat water. The binding of the complex on the surface was followed spectrally at different contact time intervals. Formed surface species, TiO$_2$:Co$^{II}$, was identified with instrumental measurements such as FTIR, DRS, PL, PXRD, EDX, XRF and SEM analysis. These studies help understand the implantation metal ion on the surface. DRS confirms the doping of metal ion into the lattice of anatase. SEM images implies a restriction in agglomeration of particles due to Co(II) penetration into the TiO$_2$. The crystal structure and surface property of Co:TiO$_2$ nanoparticle was characterized by PXRD, SEM-EDX and XRF techniques.**

**Keywords: Surface affinity; complex adduct; Co:TiO$_2$ nanomaterials; surface morphology**

## I. INTRODUCTION

Metal doped semiconductor-based photocatalysts are promising materials that have applications in energy production and environmental protection. The applications include hydrogen production, air and water purification, and hazardous waste remediation. Among various photocatalysts, $TiO_2$ has been considered as the most promising candidate because of its biological and chemical inertness, non-toxicity and long-term stability against photo- and chemical-corrosion [1]. Insertion of cobalt in the nanocrystalline $TiO_2$ samples could be responsible for the ferromagnetism [2,3]. Cobalt doped anatase nanoparticles can be used as a good photocatalyst and in spintronics. Therefore we prepared and characterized cobalt(II) implanted anatase particle using adsorption method.

## II. EXPERIMENTAL

### 2.1. Materials and methods

$CoCl_2.6H_2O$, 4-picoline (AR), nanocrystalline anatase and spectral grade KBr were purchased from Sigma Aldrich and used as received. All other chemicals were purchased from Himedia and SD Fine Chemicals (India). Analytically pure crystals of [Co$^{II}$(*4*-pic)$_4$Cl$_2$], (where *4*-pic = *4*-picoline) adsorbate was synthesized by a modified procedure and recrystallized from ethanol [4].

### 2.2. Instrumentation methods

Electronic absorption spectral studies were undertaken on a double beam spectrophotometer (Shimadzu model 2450, Japan) with integrating sphere attachment (ISR-2200). The FT-IR spectral investigations in the range 4000-400 cm$^{-1}$ were carried out on a Thermo Nicollet-6700 FT-IR instrument (KBr pellet method). Room temperature photoluminenescence (PL) was recorded with spectroflurophotometer by Horiba-JobinYvon, model SPEX-SF13-11 spectroflourimeter. Adsorption experiments were carried out in Technico cooling water bath shaker at room temperature with six different time intervals (0, 5, 10, 15, 20 and 240 min). X-ray fluorescence measurements were carried out using wavelength dispersive X-ray Fluorescence Spectrometer (WD-XRF); Make: Bruker, Model: S4 PIONEER. Powder X-ray Diffraction (PXRD) patterns were recorded in the X'PERT diffractometer employing Cu-K radiation; the wavelength of the X-ray source was = 1.541 Å. The surface morphology of the samples was investigated by scanning electron microscopy (SEM) (Hitachi, Model: S-3400N).

### 2.3. Adsorption method

About 0.1 g of the complex [Co$^{II}$(*4*-pic)$_4$Cl$_2$] was taken in a 125 mL stoppered bottle. The complex was dissolved in 70 mL of water. To this 10 mL of 1M sodium nitrate was added. Nano-$TiO_2$ (0.2 g) was added to the above solution and then the entire solution was placed in a Technico cooling water bath shaker for about 240 min at room temperature. The adsorption of cobalt(II) complex on nano-$TiO_2$ was followed at

different time intervals such as 0, 5, 10, 15, 20 and 240 min. The filtrate solutions centrifuged after definite time intervals were subjected to electronic absorption spectral analysis. The adsorbent solid (nano-TiO$_2$) was removed by centrifuging at various time intervals to understand the surface affinity of the complex ion. FTIR, DRS, PL, PXRD, SEM measurements were made on the dried solid samples obtained from adsorption experiments. The amount of cobalt adsorbed onto the adsorbent TiO$_2$ was determined by EDX and XRF measurements.

## III.    RESULTS AND DISCUSSION

### 3.1.    Adsorption of [Co(*4*-pic)$_4$Cl$_2$] on nano-TiO$_2$

Surface affinity of the Co(II)-4-picoline complex on nano-TiO$_2$ is dependent upon the concentration of the complex, contact time, dosage of adsorbent, pH and various percentage of 2-propanol/water binary mixed solvent (0 to 30 %). Thermodynamically adsorption Methodology steps were carried out by following trends (1) Complex:surface species, [Co(*4*-pic)$_4$Cl$_2$]:TiO$_2$ (ii) Surface:complex adduct and finally *x*% Co(II):TiO$_2$ surface complex species are formed.

The adsorption efficiency (Fig. 1(a)) is found to increase as the concentration of complex is increased in the solution. Similarly, the adsorption efficiency increases with respect to an enhancement in adsorbent dosage, which is visible 50-200 mg level (Fig. 1(b)). However, at the dosage level of 250-300 mg there is a decrease this may be due to desorption process. Since the dosage of the adsorbent material determined as above, accounted for the maximum removal of adsorbent, this was taken as the optimum condition for further adsorption studied using nano-TiO$_2$. The adsorption characteristics of nano-TiO$_2$ determined at various pH 3.12, 5.18, 6.01, 7.61, 8.58 and 9.10 against the contact time is depicted in Fig. 1(c). Adsorption of cobalt(II) complex ions increased appreciably with increase of pH from 3.12 to 9.10 and consistent with reported earlier [5]. That is adsorption is high in a basic medium (pH   7) while it is less in an acidic medium (pH < 7). Fig. 1(d) illustrates a linear relationship of adsorption efficiency, AE (%) of Co(II) complex adsorption on nano-TiO$_2$ particle as a function of 2-propanol content. This implies the observed adsorption efficiency of formation of nano-TiO$_2$:Co(II) surface species.
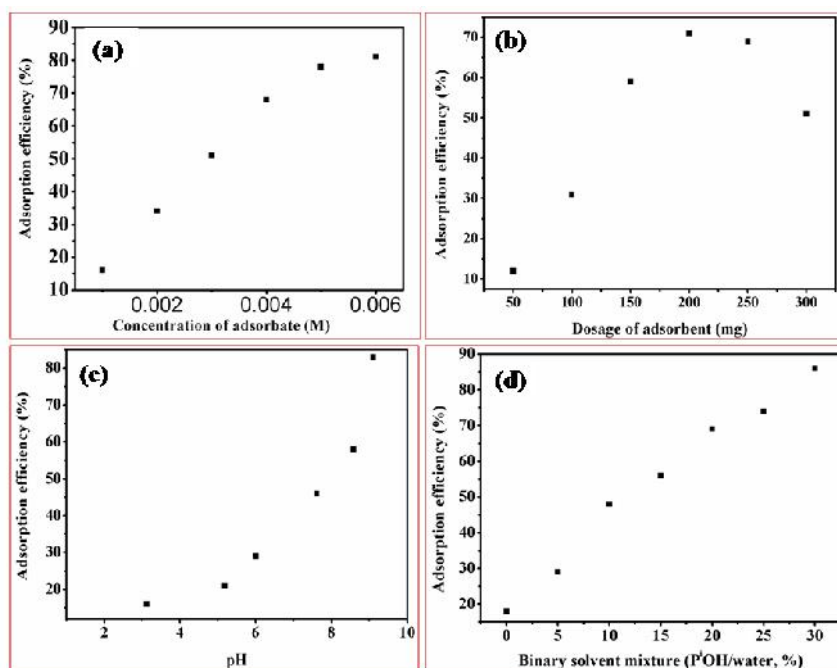


**Figure 1** (a) concentration of adsorbate (b) dosage of absorbent, (c) pH and (d) solvent variations recorded for the Co$^{II}$(*4*-pic)$_4$Cl$_2{}^{2+}$ complex adsorption on nano-TiO$_2$ in water at various time intervals at 298 K.

### 3.2.    Spectral analysis of *x*%Co:nano-TiO$_2$

Vibration spectral peaks observed between 450 - 600 cm$^{-1}$ can be assigned to the Ti-O-Ti bond as shown in Fig. 2(a). Both the pure and Co-doped nano-TiO$_2$ showed a characteristic band at 511 cm$^{-1}$ corresponding to a Ti-O bond of the anatase phase. Ti-O vibration tends to shift to lower energy region as Co content in nano-TiO$_2$.

The DRS of undoped anatase showed high reflectance, and cobalt(II) doped samples absorb more effectively in the range of 580-600 nm.
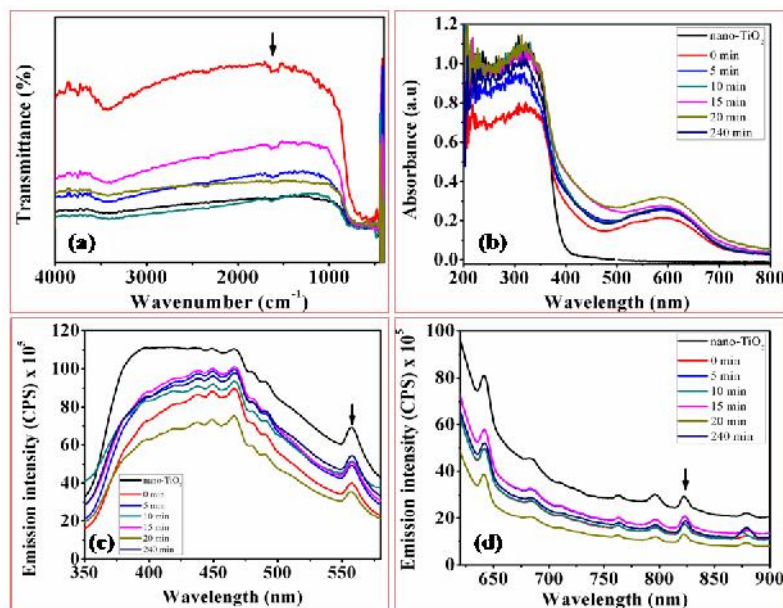


**Figure 2** (a) FTIR (in KBr) (b) DRS, (c) PL at $_{exc}$ = 310 nm and (d) PL at $_{exc}$ = 585 nm spectrums of complex:surface adduct, $Co^{II}(4\text{-pic})_4Cl_2$/nano-$TiO_2$ in pure water system at contact time intervals.

Nano-$TiO_2$ with low cobalt density absorbs at 588 nm, and the $_{max}$ shifts towards ~592 nm (Fig. 2(b)). The variation in the band gap energy of $TiO_2$ with $Co^{2+}$ concentration is shown in Table 1. Undoped $TiO_2$ nanoparticle has a larger indirect band gap energy (2.97 eV) and direct band gap energy (3.29 eV) than that of bulk (3.20 eV), which is quite expected due to quantum confinement effect. But, after cobalt doping the band gap energy is reduced to 3.18 eV and 2.99 eV for 0.41 and 1.64 (atom %) $Co^{2+}$, respectively [6].

**Table 1** Band gap energy values for x%Co/nano-$TiO_2$ obtained from photocatalysed reduction of $Co^{II}(4\text{-pic})_4Cl_2$/nano-$TiO_2$ in neat water at various time intervals.

| abbreviation of sample | direct band gap energy (eV) | indirect band gap energy (eV) | absorption edge (nm) | $_{max}$ (nm) | $_{max}$ (nm) |
|---|---|---|---|---|---|
| nano-$TiO_2$ | 3.29 | 2.97 | 407 | 307 | - |
| nano-$TiO_2$:Co, 0.44 atm. % | 3.18 | 2.76 | 468 | 308 | 588 |
| nano-$TiO_2$:Co, 0.41 atm. % | 3.06 | 2.52 | 484 | 310 | 592 |
| nano-$TiO_2$:Co, 0.50 atm. % | 2.99 | 2.48 | 477 | 307 | 590 |
| nano-$TiO_2$:Co, 2.44 atm. % | 3.05 | 2.32 | 500 | 310 | 588 |
| nano-$TiO_2$:Co, 1.63 atm. % | 3.01 | 2.33 | 485 | 313 | 592 |
| nano-$TiO_2$:Co, 1.64 atm. % | 2.99 | 2.48 | 480 | 310 | 590 |

From photoluminescence measurement only reduction in emission intensity is found for the cobalt doped samples compared to undoped sample. In our case we have not found any noticeable shifting of emission peaks (Fig. 2(c),(d)). Incorporation of Co(II) in nano-$TiO_2$ only decreases the emission intensity by forming large number of nonradiative centers [6], which act as luminescence quencher. Thus, we can conclude the decrease in the emission intensity as a collective contribution from dopants nonradiative centers produced on doping, poor crystallinity of doped samples, and oxygen defects created on $Ti^{4+}$ substitution by $Co^{2+}$.

3.3.    Structural, surface and quantitative analysis of x%Co:nano-$TiO_2$

X-ray diffraction patterns of the undoped and cobalt doped $TiO_2$ samples are presented in Fig. 3. The nanocrystalline anatase structure was confirmed by (1 0 1), (0 0 4), (2 0 0), (1 0 5) and (2 1 1) diffraction peaks [2,7,8]. The XRD patterns of anatase have a main peak at $2\theta$ = 25.2º corresponding to the 101 plane (JCPDS 21-1272). The XRD patterns didn't show any Co phase indicating that Co ions uniformly dispersed among the anatase crystallites. The average particle size was estimated from the Scherrer equation on the

anatase diffraction peaks. Average crystal sizes of nano-$TiO_2$ and Co:nano-$TiO_2$ were calculated to be around 21 nm and 26-38 nm, respectively.
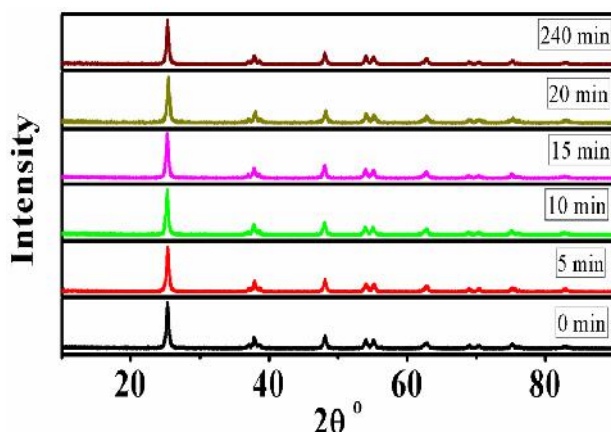


**Figure 3** Powder XRD pattern of x%Co:nano-$TiO_2$ isolated from adsorption reaction of $Co^{II}$(*4*-pic)$_4$Cl$_2$:nano-$TiO_2$.

From SEM-EDX analysis of the catalyst isolated from reaction that, formation of $Co^{II}$(pic)$_4$Cl$_2$/nano-$TiO_2$ surface compound is due to surface-coordination sphere affinity. Such compound can be selectively reduced and recovered, secondly, the surface species has been converted into x%Co:Nano-$TiO_2$ compound. EDX spectrum is useful in understanding the uptake of complex ion by the surface (Fig. 4). These results confirmed the existence of Co(II) in the solid catalysts [9].
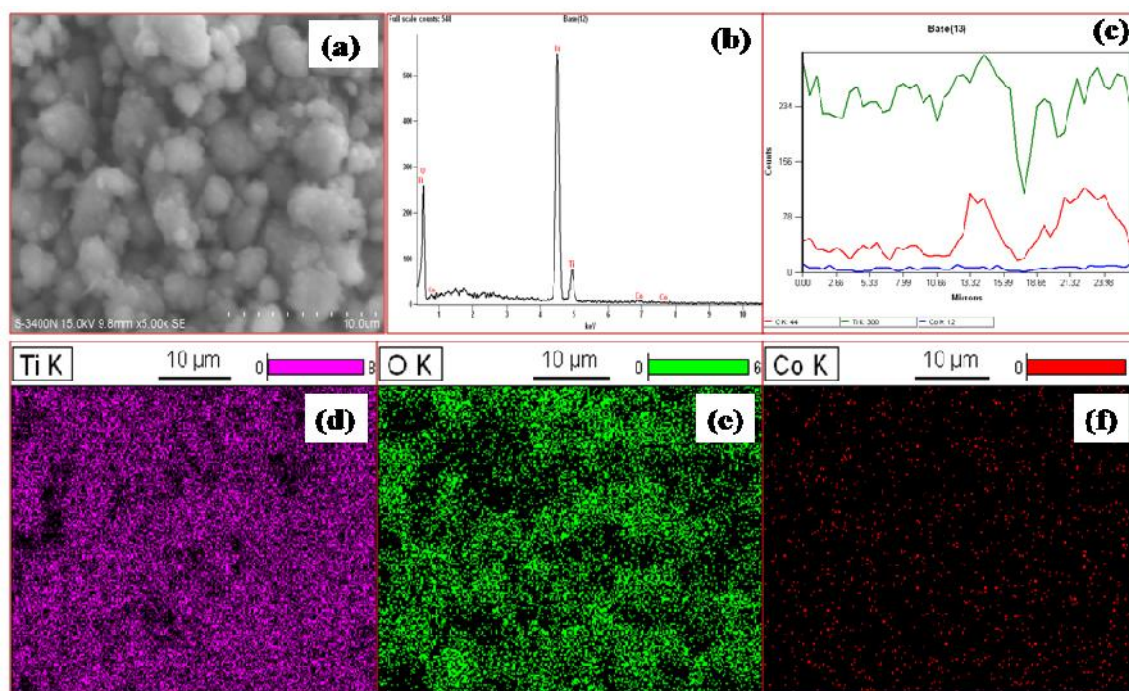


**Figure 4** *(A) SEM images and (B) EDX spectra, (c) line spectra and (d)-(f) mapping of pure x%Co:nano-$TiO_2$ particles collected from adsorption reaction $Co^{II}$(pic)$_4$Cl$_2$:nano-$TiO_2$ in neat water at 20 min.*

Therefore, it may be concluded that Co(II) ions are dispersed on the anatase crystallites. SEM micrograph of the pure nanocrystalline $TiO_2$ particles and cobalt doped nano-$TiO_2$ particles are shown in Fig. 4(a). The undoped titania consists of a poly disperse mixture of small particles (~28 nm) and coarse grains (~110 nm) [2]. The doped titania powders are composed of particles under ~85 nm. However, the doped titania exhibit some tendency to agglomeration. EDX and XRF spectral data are presented in Table 2 in which the concentration of cobalt loaded on the solid with respect to different contact

TABLE 2 EDX and XRF quantitative analysis of the $x(at.\%)$Co(II):TiO$_2$ at 298 K.

| Contact time (min.) | EDX Content, (Atm. %) | | | XRF Content, (Atm. %) | | |
|---|---|---|---|---|---|---|
| | Ti | Co | O | Ti | Co | O |
| nano-TiO$_2$ | 33.33 | - | 66.67 | 59.69 | - | 40.31 |
| 0 | 27.32 | 0.44 | 72.25 | 58.73 | 1.18 | 39.60 |
| 5 | 37.93 | 0.41 | 61.66 | 58.31 | 1.24 | 39.60 |
| 10 | 26.93 | 0.50 | 72.56 | 58.71 | 1.19 | 39.60 |
| 15 | 27.09 | 2.44 | 70.46 | 58.66 | 1.78 | 39.60 |
| 20 | 23.75 | 1.63 | 74.62 | 58.64 | 1.18 | 39.60 |
| 240 | 33.83 | 1.64 | 64.54 | 58.66 | 1.23 | 39.60 |

time are found. The intense peak is assigned to the nano-TiO$_2$ and the less intense one to the surface TiO$_2$. The peaks of Co are distinct in Fig. 4(b). In order to investigate the distribution of Co in the doped samples, SEM elemental line scan spectra and mapping was performed (Fig. 4(c)-(f). The corresponding elemental maps show the expected spatial distribution of Co confirming the insertion of Co over the entire volume of the sphere [2,10,11].

## II. CONCLUSION

In this investigation, it has been found that cobalt(II) complex surface interaction leads to the formation of nano-TiO$_2$:Co(II) surface species, that can be identified by FTIR, DRS, SEM-EDX, PXRD and XRF analysis. Co$^{II}$($4$-pic)$_4$Cl$_2$ is preferably adsorbed on nano-TiO$_2$ to form $x$%Co(II):nano-TiO$_2$ surface species. DRS result indicates the reduction in band gap values for Co(II) doped nano-TiO$_2$. It is also clear that the band gap decreases with increase in Co content in nano-TiO$_2$. It is concluded that the removal of metal ion in the form of complex is coordination structure dependent, hence, seems more specific in doping the anatase lattice.

## Acknowledgment

## References

[1] Q. Meng, T. Wang, E. Liu, X. Ma, Q. Ge and J. Gong, "Understanding Electronic and Optical Properties of Anatase TiO$_2$ Photocatalysts co-Doped with Nitrogen and Transition Metals," Phys. Chem. Chem. Phys., vol. 15, pp. 9549-9561, 2013.

[2] K. Anbalagan, "UV-Sensitized Generation of Phasepure Cobalt-Doped Anatase: Co$_x$Ti$_{1-x}$O$_{2-}$ Nanocrystals with Ferromagnetic Behavior Using Nano-TiO$_2$/cis [Co$^{III}$(en)$_2$(MeNH$_2$)Cl]$^{2+}$," J. Phys. Chem. C, vol.115, pp. 3821-3832, 2011.

[3] L. C. J. Pereira, M. R. Nunes, O. C. Monteiro, and A. J. Silvestre, "Magnetic properties of Co-doped TiO$_2$ Anatase Nanopowders," Appl. Phys. Lett., vol. 93, pp. 222502-1-3, 2008.

[4] A. S. Ganeshraja and K. Anbalagan, "Participation of Nanocrystalline TiO$_2$ Surface in the Electron Transfer between Semiconductor Solid and Adsorbed Cobalt(III)-$R$py Complex," Nano Systems: Phys. Chem. Math., vol. 4, pp. 276-287, 2013..

[5] K. Anbalagan, J.C. Juliet, "Adsorption of Chromium(VI) Ion onto Activated Amla Dust: Adsorption Isotherms and Kinetics," Indian J. Chem., vol. 43A, pp. 45-50, 2004.

[6] B. Choudhury, and A. Choudhury, "Luminescence Characteristics of Cobalt doped TiO$_2$ Nanoparticles" J. Luminescence, vol. 132, pp. 178–184, 2012.

[7] A. S. Ganeshraja and K. Anbalagan, "Synthesis and Characterization of Co/nano-TiO$_2$ using UV-light Irradiation of Co$^{II}$(pic)$_4$Cl$_2$ Complex with Nano-TiO$_2$," Int. J.Nanotech. Appl., vol. 6, pp. 127–131, 2012.

[8] K. Anbalagan and A. S. Ganeshraja, "Single Crystal Structure Refinement of Co$^{II}$(C$_9$H$_7$N)$_2$Br$_2$ and its Surface Affinity on Titanium Dioxide using PXRD, SEM and XRF Measurements," J. Indian Chem. Soc., vol. 90, pp. 143-152, 2013.

[9] M. Hamadanian, A. Reisi-Vanani, and A. Majedi, "Sol-Gel Preparation and Characterization of Co/TiO$_2$ Nanoparticles: Application to the Degradation of Methyl Orange," J. Iran. Chem. Soc., vol. 7, pp. S52-S58, 2010.

[10] K. Anbalagan, A.S. Ganeshraja, C. Maharaja Mahalakshmi, "Excited Nanoscale-TiO$_2$ Induced Interfacial Electron Transfer Reaction of Redox Active Cobalt(III)-Alkyl Amine Complex and the Solid Surface," Mater. Chem. Phys. vol. 134, pp. 747-754, 2012.

[11] K. Anbalagan, A. S. Ganeshraja, "Electron-rich Ligand Modified, Ferromagnetic Luminescent cis-[Co$^{III}$(en)$_2$(RNH$_2$)Cl]Cl$_2$ Complexes and their Electrochemical Reduction Behavior," Inorg. Chem. Commun., vol. 37, pp.59-65, 2013.